Optical spectroscopy of Nd^{3+} ions in poly(acrylic acid)

2006 J. Phys.: Condens. Matter 18 7951

(http://iopscience.iop.org/0953-8984/18/34/008)

INSTITUTE OF PHYSICS PUBLISHING JOURNAL OF PHYSICS: CONDENSED MATTER

J. Phys.: Condens. Matter **18** (2006) 7951–7959 doi:10.1088/0953-8984/18/34/008

Optical spectroscopy of Nd^{3+} ions in poly(acrylic acid)

F Ramos-Lara[1], A Lira C[1], M O Ramírez[2], M Flores[1], R Arroyo[3] and U Caldiño[2,4]

[1] Departamento de Física, Universidad Autónoma Metropolitana-Iztapalapa, PO Box 55-534, 09340 México, DF, Mexico
[2] Departamento de Física de Materiales, Universidad Autónoma de Madrid, Cantoblanco, 28049 Madrid, Spain
[3] Departamento de Química, Universidad Autónoma Metropolitana-Iztapalapa, PO Box 55-534, 09340 México, DF, Mexico

E-mail: cald@xanum.uam.mx

Received 8 June 2006, in final form 12 July 2006
Published 7 August 2006
Online at stacks.iop.org/JPhysCM/18/7951

Abstract

Nd^{3+} dissolved in solid poly(acrylic acid) was synthesized by polymerization of the monomer partially neutralized with neodymium hydroxide in aqueous solution. The monomer modification and the coordination of ligands to Nd^{3+} were confirmed by ^1H NMR spectroscopy. The measured oscillator strengths for transitions from the ground state to the main excited state manifolds compared favourably with calculated electric dipole oscillator strengths. The spontaneous emission rates, the fluorescence branching ratios and the stimulated emission cross sections of the $^4F_{3/2} \rightarrow {}^4I_{9/2}$, $^4F_{3/2} \rightarrow {}^4I_{11/2}$ and $^4F_{3/2} \rightarrow {}^4I_{13/2}$ transitions, as well as the radiative lifetime and the quantum efficiency of the $^4F_{3/2}$ emitting level, were determined.

1. Introduction

The optical properties of Nd^{3+} in various materials have been extensively studied, because neodymium is the most common activator ion in laser crystals, owing to its intense luminescence, and it is, therefore, of considerable interest in quantum electronics and its applications [1–4]. Furthermore, the Nd^{3+} ion is a typical light lanthanide ion that is very convenient for spectral measurements [5].

In the last decade or so, an increasing number of papers have been addressed to studying the use of polymeric materials as hosts for rare earth (RE) ions, due to their important technological applications [6–8]. Much of this interest has centred on organic materials, because they may exhibit nonlinear optical properties that surpass those of the inorganic compounds. Materials with large optical nonlinearities can be useful for frequency conversion and the modulation

[4] On sabbatical leave from: Departamento de Física, UAM, Iztapalapa, PO Box 55-534, 09340 México, DF, Mexico.

of laser radiation, leading to a wide range of applications, including optical data storage, communications and optical computing systems. Moreover, organic materials can be used in films and coatings [9]. They usually offer easier and lower-cost processing, faster response time and high transparency [10, 11].

The purpose of this paper is to present data of a systematic investigation of the ^{1}H NMR, luminescence and optical absorption spectra at room temperature of Nd^{3+} in poly(acrylic acid) (PAA). The Judd–Ofelt parameters were determined to obtain more information about the optical spectroscopy of the trivalent neodymium in PAA. Such parameters allowed us to calculate the electric dipole oscillator strengths, which compared favourably with the measured oscillator strengths. Then, the radiative emission probabilities, the branching ratios and the stimulated emission cross sections of the $^4F_{3/2} \rightarrow {}^4I_{9/2}$, $^4F_{3/2} \rightarrow {}^4I_{11/2}$ and $^4F_{3/2} \rightarrow {}^4I_{13/2}$ transitions, as well as the radiative lifetime and the quantum efficiency of the $^4F_{3/2}$ level, were determined.

2. Experimental details

Acrylic acid (AA) (99%, Aldrich Chemical Co.) was previously purified by distillation at reduced pressure. 1 mol of AA was dissolved in de-ionized water at a molar ratio of 1:20. Then, different amounts of freshly prepared neodymium hydroxide (from neodymium (III) nitrate (99%, Aldrich Chemical Co.) and potassium hydroxide (99%, Aldrich Chemical Co.)) were added to the solution while stirring. An amount of 10^{-3} mol of potassium persulfate (99 + %, Aldrich Chemical Co.) was added to the solution with the hydroxides completely dissolved. The reaction mixture was heated at 65–70 °C for 60 min, and then poured into Teflon containers for drying at 120 °C and under reduced pressure (20 Torr). Samples of PAA containing 3 and 5 mol% of Nd^{3+} in the starting solution were prepared.

The ^{1}H NMR spectra were performed at 500.13 MHz by means of a Bruker DMX500 NMR spectrometer. Measurements of the chemical shifts were obtained from 2,2-dimethyl-2-silapentane-5-sulfonic acid, which was added to the solutions as an internal standard. The absorption spectrum was carried out on a Varian model Cary 5 spectrophotometer. The emission spectra were recorded by exciting the sample with a continuous wave (CW) Ti:sapphire laser (Spectra Physics, model 3900) pumped by an Ar^+ laser (Spectra Physics, model 2040E). The pulsed excitation required for lifetime measurements was achieved by means of a chopper PAR EG&G model 196. The emission from the sample was dispersed by a 500 M SPEX monochromator and detected with a cooled photomultiplier R5108. A lock-in amplifier (PAR EG&G model 5209) was used to improve the signal-to-noise ratio. Lifetime data were processed by a Le Croy model LT372 digitizing oscilloscope.

The spectroscopic measurements were performed in thermoformed polymer discs. Discs of the same thickness were obtained from a constant quantity of polymer, finely powdered, and thermoformed into two Mylar sheets at 120–130 °C and under a pressure of 5 kg cm^{-2}. All the measurements were obtained at room temperature and immediately after the polymer discs were thermoformed to avoid excessive polymer hydration.

3. Results and discussion

3.1. Characterization

The ^{1}H NMR spectra of AA pure and partially neutralized in the vinylic region are displayed in figure 1. The AA pure spectrum has been reported previously and consists of three quadruplets centred at 6.42 ppm (*cis* proton), 6.17 ppm (germinal proton) and 6.01 ppm (*trans* proton) [12]. The spectra of the samples with Nd^{3+} show a small signal broadening and a low-field shift

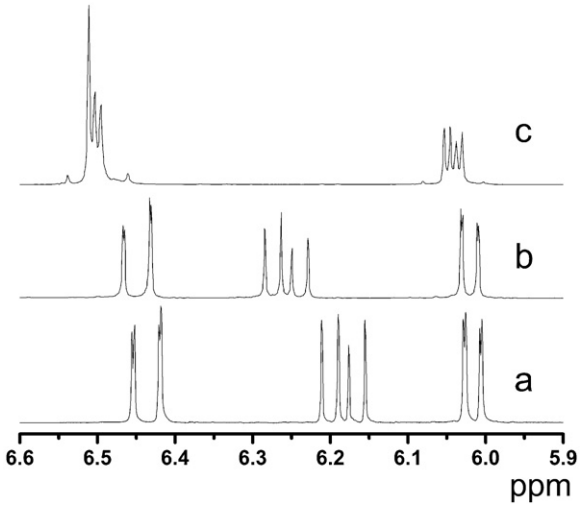

Figure 1. ^{1}H NMR spectra of (a) pure acrylic acid [12] and containing (b) 3 mol% and (c) 5 mol% of Nd^{3+}.

relative to the pure monomer. The chemical shift in the signals of the vinylic protons increases with the concentration of Nd^{3+}. The smallest chemical shift is observed for the *trans* proton. The geminal proton signal shows the largest chemical shift. The signal shift of the geminal proton in the sample containing 5 mol% of Nd^{3+} (figure 1(c)) is so pronounced that it overlaps with the signal due to *cis* proton. This signal integrates for two protons, while the signal due to the *trans* proton integrates for one proton. The broadening and the chemical shift have been attributed to the magnetic anisotropy and electron-spin relaxation time of the Nd^{3+} ion [13]. The ^{1}H NMR spectra suggest that neodymium acrylate complexes are formed during the partial neutralization of the monomer. Such complexes seem to be completely disordered, because the polymer acts like an 'immobile' solvent in the vicinity of the coordinated Nd^{3+} ions [14]. When the polymerization is carried out, the reaction mixture becomes viscous, and after 1 h a gel is obtained. No precipitated Nd^{3+} was observed, which supports the fact that Nd^{3+} ions were incorporated into the polymer matrix. Considering that, in the neutralization process, hydroxide ions form water with the protons produced from the dissociation of AA, the only possible counter-ions in the polymer are carboxylate anions, which can be coordinated to the Nd^{3+} ions [15, 16].

3.2. Absorption

The absorption spectrum in the 300–900 nm spectral region of Nd^{3+} in PAA:Nd (3 mol%) is displayed in figure 2. The absorption peaks, corresponding to transitions from the ground state $^4I_{9/2}$ to higher-energy states inside the $4f^3$ electronic configuration of the Nd^{3+} ion, are identified in the figure. The absorption spectrum is dominated by the $^4I_{9/2} \rightarrow {}^4G_{5/2} + {}^2G_{7/2}$ transition due to the hypersensitive character of the $^4G_{5/2}$ multiplet. The absorption bands at wavelengths shorter than 300 nm could not be detected, because of the strong absorption of the host sample in the ultraviolet range.

3.3. Luminescence

Figure 3 presents emission spectra of Nd^{3+} in PAA:Nd (3 mol%) in the 840–960 nm, 1000–1120 nm and 1260–1500 nm regions. These spectra were obtained by exciting the $^4F_{5/2}$

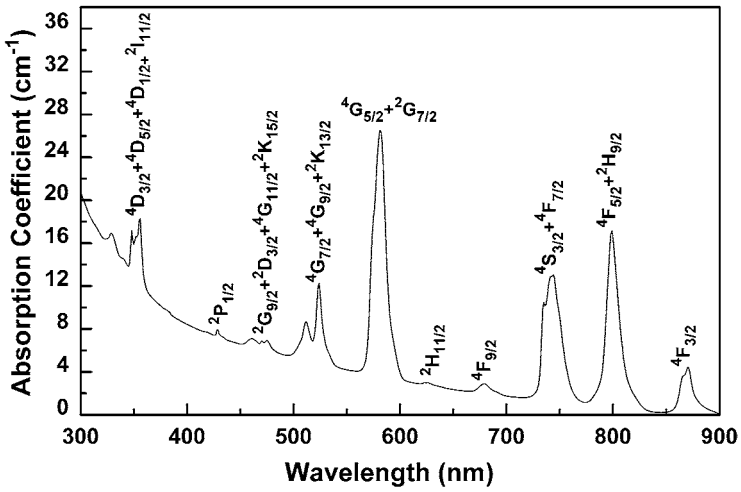

Figure 2. Absorption spectrum of Nd^{3+} in PAA:Nd (3 mol%).

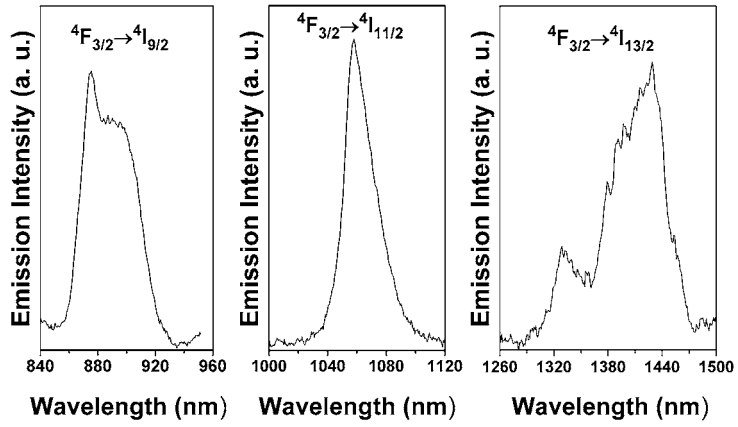

Figure 3. Emission spectra after $^4F_{5/2}$ multiplet excitation at 800 nm in PAA:Nd (3 mol%).

multiplet at 800 nm. They consist of three emission broad bands centred at around 882, 1062 and 1400 nm, which are associated with the transitions $^4F_{3/2} \rightarrow {}^4I_{9/2}$, $^4F_{3/2} \rightarrow {}^4I_{11/2}$ and $^4F_{3/2} \rightarrow {}^4I_{13/2}$, respectively. From these spectra it can be seen that the main laser line $^4F_{3/2} \rightarrow {}^4I_{11/2}$ peaks at 1058 nm. The emission $^4F_{3/2} \rightarrow {}^4I_{15/2}$ was quite weak, so that it could not be detected. In fact, the participation of the $^4F_{3/2} \rightarrow {}^4I_{15/2}$ transition in the emission of the $^4F_{3/2}$ multiplet has been found to be negligible [17, 18].

3.4. Data analysis

Judd–Ofelt (JO) analysis [19, 20] has become a standard method for calculating the parity-forbidden electric dipole radiative transition rates between various levels of rare-earth ions in a great variety of ion-host combinations [17, 18, 21]. The experimental strength values are required to estimate the phenomenological JO parameters Ω_2, Ω_4 and Ω_6 by means of a least-squares fitting. These parameters allow us to calculate the strength of any radiative transition,

as well as radiative lifetimes and fluorescence branching ratios, which are very important in the determination of stimulated emission cross sections and the efficiency of lasers and amplifiers.

According to the JO theory, the line strength for electric–dipole transitions between two manifolds defined by their angular quantum numbers J and J', S_{ed}, in an isotropic material, can be expressed in terms of the Ω_t intensity parameters:

$$S_{ed} = \sum \Omega_t |\langle [L, S]J \| U^t \| [L', S']J' \rangle|^2, \qquad t = 2, 4, 6, \tag{1}$$

where the matrix elements $\langle [L, S]J \| U^t \| [L', S']J' \rangle$ are doubly reduced unit tensor operators of rank t calculated in the intermediate-coupling approximation and are almost independent of the host environment. Then, the host dependence in equation (1) is taken into account through the Ω_2, Ω_4 and Ω_6 phenomenological parameters, which characterize the radiative transition probabilities within the ground configuration. These three intensity parameters are independent of the electronic quantum numbers with the ground-state configuration, and express the influence of the host on the transition probabilities, because they contain crystal-field parameters, interconfigurational radial integrals and the interaction between the central ion and the immediate environment. The values of the reduced matrix elements for the chosen absorption bands were taken from Carnall [22]. For the ion neodymium, the matrix element $\|U^2\|^2$ is large for the hypersensitive transition $^4I_{9/2} \rightarrow {}^4G_{5/2}$. A basic assumption involved in equation (1) is that all the crystal-field levels of the ground state are equally populated, i.e. transitions from all Stark levels of the $^4I_{9/2}$ multiplet are equally probable. At high enough temperature, in general at room temperature (RT), a maximum population of the Stark levels in the ground state is achieved, so that the assumption of equal population of the $^4I_{9/2}$ multiplet Stark levels is fulfilled.

The oscillator strength from the initial state J (=9/2) to a final state J', in terms of the electric dipole line strength, S_{ed}, is given by:

$$f_{calc} = \frac{8\pi^2 mc}{3h(2J+1)\bar{\lambda}} \chi_{ed} S_{ed}, \tag{2}$$

where S_{ed} is given by equation (1), $(2J + 1)$ is the degeneracy of the level, $\bar{\lambda}$ is the mean wavelength of the transition between the two manifolds, and χ_{ed} is the local field correction for the refractivity of the medium which, for an isotropic material of refractive index n, is given by:

$$\chi_{ed} = \frac{(n^2+2)^2}{9n}. \tag{3}$$

The oscillator strength for each transition from the fundamental multiplet J (=9/2) to excited J' multiplets can be determined experimentally from its corresponding integrated absorption coefficient according to the equation:

$$f_{meas} = \frac{2mc}{\alpha_f h N \bar{\lambda}^2} \int \alpha(\lambda)\, d\lambda, \tag{4}$$

where α_f is the fine-structure constant, $\alpha(\lambda)$ is the absorption coefficient (cm^{-1}) at the wavelength λ, and N is the concentration of active ions. The absorption coefficient reduces the accuracy of f_{meas} by uncertainties in the integration of the absorption bands due mainly to noise and assignment of peaks to each transition. Such uncertainties might be of the order of 5%–10%. The value estimated for the concentration of Nd^{3+} ions in PAA:Nd (3 mol%) resulted in being about 2.5×10^{20} ions cm^{-3}. The refraction index of the polymer was found to be 1.55.

The JO parameters were, then, estimated from a least-squares fitting between the measured f_{meas} and calculated f_{cal} oscillator strengths, treating Ω_t as adjustable parameters. A set of

Table 1. Measured and calculated oscillator strengths of Nd^{3+} in PAA:Nd (3 mol%). All the transitions are from the $^4I_{9/2}$ ground state to the multiplets indicated.

Multiplets	Average wavelength (nm)	$f_{meas} \times 10^{-6}$	$f_{calc} \times 10^{-6}$
$^4F_{3/2}$	868.3	2.80	3.82
$^4F_{5/2}, {}^2H_{9/2}$	800.3	16.42	15.98
$^4F_{7/2}, {}^4S_{3/2}$	743.4	17.82	18.31
$^4F_{9/2}$	676.7	0.62	1.39
$^4G_{5/2}, {}^2G_{7/2}$	580.9	43.84	43.87
$^4G_{7/2}, {}^4G_{9/2}, {}^2K_{13/2}$	519.4	14.59	11.37
$^2G_{9/2}, {}^2D_{3/2}, {}^4G_{11/2}, {}^2K_{15/2}$	467.5	2.51	2.51
$^4D_{3/2}, {}^4D_{5/2}, {}^4D_{1/2}, {}^2I_{11/2}$	352.6	15.67	17.45

eight equations for the transitions from the ground state $^4I_{9/2}$ up to the $^4D_{3/2}$, $^4D_{5/2}$, $^4D_{1/2}$, and $^2I_{11/2}$ multiplets were constructed through comparison of equation (4) with equation (2). The overlap among some multiplets was resolved by building independent Gaussian curves. The values calculated for the Ω_t are: $\Omega_2 = 1.25 \times 10^{-19}$ cm^2, $\Omega_4 = 6.44 \times 10^{-20}$ cm^2 and $\Omega_6 = 1.32 \times 10^{-19}$ cm^2. Table 1 displays the average wavelength of the transitions from the fundamental multiplet to the excited multiplets considered, and the corresponding calculated and measured oscillator strengths. The quality of our fitting was measured by the root mean square (RMS) deviation, which turned out to be equal to 9.2%. The largest electric dipole oscillator strength was found for the $^4I_{9/2} \rightarrow {}^4G_{5/2}, {}^2G_{7/2}$ transitions, which are associated with the most intense absorption band in the spectrum of figure 2. The spectroscopic quality factor $X = \Omega_4/\Omega_6$, first introduced by Kaminskii [23], is a spectroscopic parameter that is critically important in predicting the stimulated emission of the laser active medium. The value obtained for X turned out to be 0.49, which is slightly lower than those reported for other Nd^{3+}-based laser materials [18, 24, 25]. However, the ratio Ω_4/Ω_6 obtained is within the range 0.3–0.6, for which it has been reported that glasses and crystals are good candidates for laser action, considering that, within this range, the fluorescence branching ratio possesses a desirable high value for the $^4F_{3/2} \rightarrow {}^4I_{11/2}$ laser channel [26].

The JO parameters were used to calculate the total spontaneous emission probabilities, $A(J \rightarrow J')$, for the $^4F_{3/2} \rightarrow {}^4I_{9/2}$, $^4F_{3/2} \rightarrow {}^4I_{11/2}$ and $^4F_{3/2} \rightarrow {}^4I_{13/2}$ transitions, applying the following relation in terms of S_{ed}:

$$A(J \rightarrow J') = \frac{32\pi^3 c\alpha_f n^2}{3(2J+1)\bar{\lambda}^3}\chi_{ed}S_{ed}, \tag{5}$$

where the $(2J+1)$ degeneracy factor implicitly contains the assumption of equal population of all levels of the initial multiplet ($J = 3/2$). The $A(J \rightarrow J')$ radiative emission probability of the level $^4F_{3/2}$ is predominantly due to the forced electric dipole component [18, 24, 25]. The radiative lifetime can, then, be determined from the following relation:

$$\tau_{rad} = \frac{1}{\sum_{J'} A(J \rightarrow J')}, \tag{6}$$

where the sum is over all final states J'. The fluorescence branching ratios of the transitions $J \rightarrow J'$ can be determined from the ratio of the spontaneous radiative emission rate of the observed transition to the total spontaneous emission rate from the initial state:

$$\beta_{J\rightarrow J'} = \frac{A(J \rightarrow J')}{\sum_{J'} A(J \rightarrow J')} = A(J \rightarrow J')\tau_{rad}. \tag{7}$$

The radiative emission probabilities and the branching ratios of the $^4F_{3/2} \rightarrow {}^4I_{9/2}$, $^4F_{3/2} \rightarrow {}^4I_{11/2}$ and $^4F_{3/2} \rightarrow {}^4I_{13/2}$ transitions, as well as the radiative lifetime of the $^4F_{3/2}$ level, are

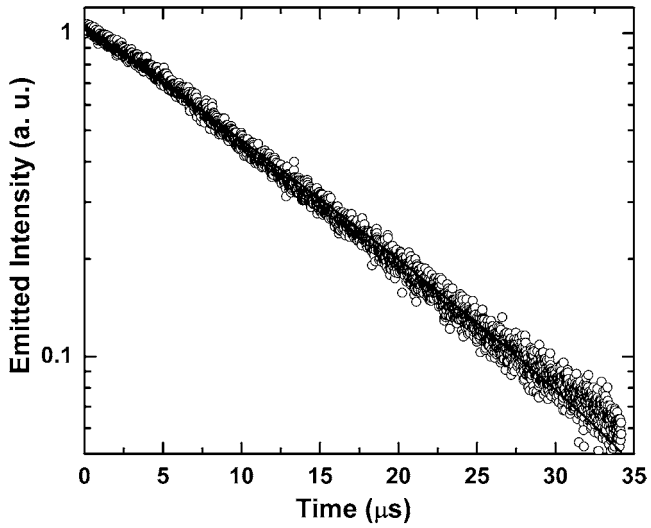

Figure 4. Time dependence of the 1058 nm Nd^{3+} emission obtained with $^4F_{5/2}$ multiplet excitation at 800 nm in PAA:Nd (3 mol%).

Table 2. Branching ratios $\beta_{J\to J'}$ and radiative emission probabilities $A(J \to J')$ for the $^4F_{3/2} \to {}^4I_{9/2,11/2,13/2}$ transitions, and radiative lifetime τ_{rad} of the $^4F_{3/2}$ level in PAA:Nd (3 mol%).

Transition	Average wavelength (nm)	$\beta_{J\to J'}$	$A(J \to J')$ (s^{-1})	τ_{rad} (μs)
$^4F_{3/2} \to$				102
$^4I_{9/2}$	882.9	0.20	1927.5	
$^4I_{11/2}$	1064.0	0.72	7070.4	
$^4I_{13/2}$	1408.0	0.08	844.4	

listed in table 2. The main laser transition $^4F_{3/2} \to {}^4I_{11/2}$ has the greatest branching ratio (0.72). The branching ratio associated with the $^4F_{3/2} \to {}^4I_{15/2}$ transition has usually been found to be zero [17, 18].

The overall quantum efficiency, η, of the $^4F_{3/2}$ level was estimated using the value determined for τ_{rad} (102 μs) and the τ_f fluorescence lifetime measured, which was found to be 13 μs (figure 4). Thus, η was found to be about 13% as a consequence of a quite large non-radiative decay rate ($W_{nr} = 1/\tau_f - 1/\tau_{rad} = 7.6 \times 10^4\ s^{-1}$) from the $^4F_{3/2}$ state.

3.5. Stimulated emission cross section

The stimulated emission cross section can be determined from the emission spectrum using the Füchtbauer–Ladenburg relation once the corresponding $\beta_{J\to J'}$ branching ratio is known [27]:

$$\sigma_{em}(\lambda) = \frac{\lambda^5 \beta_{J\to J'} I(\lambda)}{8\pi n^2 c \tau_{rad} \int \lambda I(\lambda)\, d\lambda}, \tag{8}$$

where $I(\lambda)$ is the emission intensity as a function of the λ emission wavelength.

Figure 5 presents the spectral dependence of the stimulated emission cross section for the $^4F_{3/2} \to {}^4I_{9/2}$, $^4F_{3/2} \to {}^4I_{11/2}$ and $^4F_{3/2} \to {}^4I_{13/2}$ transitions, which was determined from the corresponding emission spectra obtained with $^4F_{5/2}$ multiplet excitation at 800 nm. As

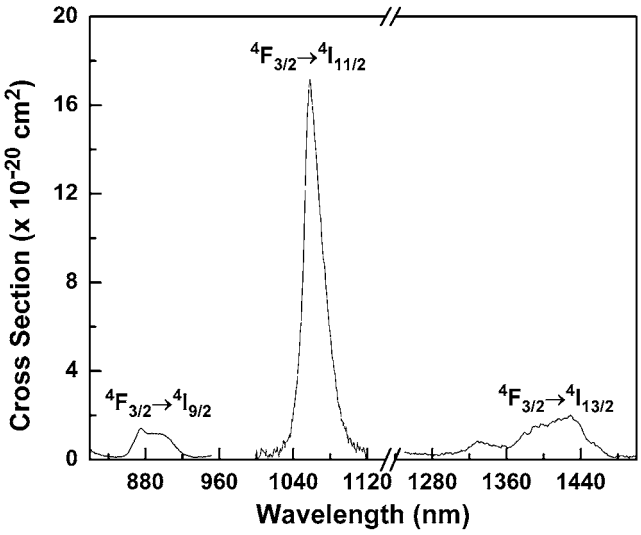

Figure 5. Spectral dependence of the stimulated emission cross section for the $^4F_{3/2} \rightarrow {}^4I_{9/2}$, $^4F_{3/2} \rightarrow {}^4I_{11/2}$ and $^4F_{3/2} \rightarrow {}^4I_{13/2}$ transitions in PAA:Nd (3 mol%).

expected, the stimulated emission cross section for the main laser transition $^4F_{3/2} \rightarrow {}^4I_{11/2}$ turned out to be the highest one. The peak cross section, calculated at $\lambda = 1058$ nm, turned out to be 17.2×10^{-20} cm^2, which is similar to those reported for other Nd^{3+}-based laser materials [24, 25, 28].

4. Conclusions

Nd^{3+}-doped poly (acrylic acid) was synthesized by polymerization of acrylic acid partially neutralized with neodymium hydroxide. ^{1}H NMR spectra revealed that neodymium acrylate complexes are formed during the partial neutralization of the monomer. Measured oscillator strengths have been compared with calculated strengths for the same transitions and the results are found to be within the limits of accuracy of the JO analysis. The peak cross section of the main laser emission $^4F_{3/2} \rightarrow {}^4I_{11/2}$, calculated at $\lambda = 1058$ nm, turned out to be 17.2×10^{-20} cm^2, which is similar to those reported for other Nd^{3+}-based laser materials. However, the quantum efficiency of the $^4F_{3/2}$ emitting level is low (13%) as a consequence of a large non-radiative decay probability.

Acknowledgments

This work was supported by the CONACyT under project contract 43016-F and by the CYTED subprogram VIII-12. U Caldiño thanks the Ministerio de Educación y Ciencia of Spain for sabbatical support (SAB 2004-002). We are also grateful to Dr D Jaque (Departamento de Física de Materiales, Universidad Autónoma de Madrid) for valuable discussions.

References

[1] Kaminskii A A 1991 *Ann. Phys.* **16** 639
[2] Katsumata T, Hanamori K, Akiyama Y and Nobe Y 1995 *Mater. Res. Bull.* **30** 19

[3] Caldiño G U, Voda M, Jaque F, García Solé J and Kaminskii A A 1993 *Chem. Phys. Lett.* **213** 84
[4] Ambrazyavichyus G A, Babonas G A, Bandorev A D and Leonov E I 1981 *Opt. Spectrosk.* **51** 184
[5] Bukietynska K and Mondry A 1985 *Inorg. Chim. Acta* **110** 1
[6] Slooff L H, van Blaaderen A, Polman A, Hebbink G A, Klink S I, van Veggel F C J M, Reinhoudt D N and Hofstraat J W 2002 *J. Appl. Phys.* **91** 3955
[7] Xu X, Ming H and Zhang Q 2001 *Opt. Commun.* **199** 369
[8] Weber M J, Meyers J D and Blackburn D H 1981 *J. Appl. Phys.* **52** 2944
[9] Rajagopalan P, Tsatsas A T and Risen W M Jr 1996 *J. Polym. Sci.* B **34** 151
[10] Dreger Z A, Yang G, White J O, Li Y and Drickamer H G 1998 *J. Phys. Chem.* B **102** 4380
[11] Okamoto Y 1987 *J. Macromol. Sci. Chem.* A **24** 455
[12] Lira C A, Flores M, Arroyo R and Caldiño U 2006 *Opt. Mater.* **28** 1171
[13] Nieboer E 1975 *Structure and Bonding* vol 22 (New York: Springer) p 1
[14] Carlos L D and Videira A L L 1997 *Chem. Phys. Lett.* **264** 57
[15] Yang M, Ling Q, Hiller M, Fun X, Liu X, Wang L and Zhang W 2000 *J. Polym. Sci.* A **38** 3405
[16] Flores M, Rodríguez R and Arroyo R 1999 *Mater. Lett.* **39** 329
[17] Ramos F, Loro H, Camarillo E, García-Solé J, Kaminskii A A and Caldiño G U 1999 *Opt. Mater.* **12** 93
[18] Ramos F, Jaque D, Romero J, García-Solé J and Caldiño G U 1999 *J. Phys.: Condens. Matter* **11** 3201
[19] Judd B R 1962 *Phys. Rev.* **127** 750
[20] Ofelt G S 1962 *J. Chem. Phys.* **37** 511
[21] Henderson B and Imbush G F 1989 *Optical Spectroscopy of Inorganic Solids* ed B Henderson and G F Imbush (Oxford: Clarendon)
[22] Carnall W T, Fields P R and Wybourne B G 1965 *J. Chem. Phys.* **42** 3797
[23] Kaminskii A A 1975 *Zh. Tekh. Fiz. Pis.* **1** 256
[24] Jaque D, Enguita O, Caldiño U, Ramírez M O, García-Solé J, Zaldo C, Muñoz-Santiuste J E, Jiang A D and Luo Z D 2001 *J. Appl. Phys.* **90** 561
[25] Romero J J, Jaque D, Ramos Lara F, Boulon G, Guyot Y, Caldiño G U and García Solé J 2002 *J. Appl. Phys.* **91** 1754
[26] Sardar D K, Velarde-Montecinos R C and Vizcarra S 1993 *Phys. Status Solidi* a **136** 555
[27] Payne S A, Chase L L, Smith L-K, Kway L and Krupke W F 1992 *IEEE J. Quantum Electron.* **28** 2619
[28] Jaque D, Capmany J, Luo Z D and García Solé J 1997 *J. Phys.: Condens. Matter* **9** 9715